RSC Advances

PAPER

View Article Online
View Journal | View Issue

Cite this: *RSC Adv.*, 2024, **14**, 11977

Green and efficient magnetic micro-solid phase extraction utilizing tea waste impregnated with magnetic nanoparticles for the analysis of ibuprofen in water samples by using UV-vis spectrophotometry†

Yagulan Muniandy, [a] Sharifah Mohamad*[ab] and Muggundha Raoov [ab]

A green method based on magnetic micro-solid phase extraction (MNP-TW-μ-SPE) of tea waste impregnated with magnetic nanoparticles (MNP-TW) was developed for the extraction of ibuprofen (IBP) in water samples prior to UV-Vis spectrophotometric analysis. Experimenting parameters that affect the extraction efficiency of IBP, such as pH of the sample solution, sorbent dosage, extraction time, ionic strength, volume of the sample, type of desorption solvent, desorption time, and desorption volume, were studied and optimized in detail. The characterization studies for the MNP-TW were carried out by Fourier transform infrared spectroscopy (FTIR), X-ray diffraction spectrometry (XRD), field emission scanning electron microscopy (FESEM), transmission electron microscopy (TEM), Brunauer–Emmett–Teller (BET) analysis, a vibrating sample magnetometer (VSM), and thermogravimetric analysis (TGA). Under the optimum conditions, the linearity ranges from 30 to 700 μg L^{-1} for IBP, with determination coefficients (R^2) of 0.9983. The limit of detection (LOD) and limit of quantification (LOQ) were 9.40 μg L^{-1} and 28.50 μg L^{-1}, respectively. The method also demonstrated good precision in reproducibility (RSD ≤ 1.53%), repeatability (RSD ≤ 1.48%), and recovery (86–115%). This method represents the advantages of low solvent consumption, flexibility, and better sensitivity compared to other studies employing spectrophotometric analysis. The usage of tea waste in the extraction process presents many advantages, as it is biodegradable, versatile, and contributes to an intelligent and sustainable economic strategy projected toward a circular economy approach.

Received 5th February 2024
Accepted 27th March 2024

DOI: 10.1039/d4ra00940a

rsc.li/rsc-advances

Introduction

Recently, a class of medication known as ibuprofen (IBP) has become one of the most popular (over-the-counter) drugs used to treat pain and inflammation.[1] Overdose of this drug typically results in unfavourable side effects such as ulcers, kidney failure, and gastrointestinal bleeding, which can eventually cause sudden death. Those with weak health conditions and alcoholic practices might experience negative effects more severely.[2]

IBP is among the "emerging" unregulated pollutants that were easily introduced into water body systems and have become an environmental concern.[3] It can be found in trace amounts in sediment, groundwater, surface water, the ocean, wastewater (influent and effluent), and sewage treatment plants (STP), which indicates an inefficient treatment process.[4] Approximately more than 15% of drugs often found in environmental water samples were IBP, partly due to their hydrophilicity and stability in surface waters.[5] Therefore, there is considerable interest in the development of highly sensitive, selective, rapid, and cost-effective analytical methods for monitoring IBP.

IBP is high in demand, and many nations continue to consume it at higher rates.[2,6] At trace level, this pollutant might endanger aquatic ecosystems and human health since it can be released into the environment in many ways, such as disposal of unused medicines, patient excretions, poor sewage treatment plants from pharmaceutical manufacturing, and hospitals.[7] Continuous exposure to these bio-accumulative compounds would harm aquatic life and eventually pose a risk to other organisms, including human beings. This threatens the environment and human health, which makes it crucial to detect and determine the IBP concentration in the water samples.[8]

At trace-level concentrations, it is difficult to go down to this detection limit due to complex matrix effects. Considering this,

[a]*Department of Chemistry, Faculty of Science, Universiti Malaya, 50603, Kuala Lumpur, Malaysia*

[b]*Universiti Malaya Centre for Ionic Liquids, Department of Chemistry, Faculty of Science, Universiti Malaya, Kuala Lumpur 50603, Malaysia*

† Electronic supplementary information (ESI) available. See DOI: https://doi.org/10.1039/d4ra00940a

a precise sample preparation technique for the identification and quantification of IBP is crucial.

Quantitative analysis is of immense importance, and detection techniques such as gas chromatography, liquid chromatography, capillary electrophoresis, and voltammetry with mass spectroscopy libraries have been developed and studied. Combinations of these techniques make qualitative and quantitative analysis excellent. However, drawbacks arise when considering the excessive cost of equipment, the duration of analysis, the expertise required to operate sophisticated operations, *etc.* On the other hand, spectrophotometric methods are widely available, easily managed, faster, and less costly. It is also very convenient for on-site monitoring. However, due to the low sensitivity factor of the UV-Vis spectrophotometer, a preconcentration-separation technique is required for precise and accurate measurements.[9–11]

Therefore, the enrichment and purification of IBP have been achieved using a variety of sample preparation techniques. Drugs and their metabolites are typically determined using the liquid–liquid extraction (LLE), solid phase extraction (SPE), stir rod sorptive extraction (SRSE), dispersive liquid–liquid microextraction (DLLME), and solid phase micro-extraction (SPME) procedures.[12] Solid phase extraction (SPE) has the advantages of providing high enrichment factors, exquisite selectivity, and high recovery, making it one of the most vital and dependable approaches. However, the traditional SPE approach has drawbacks such as loss of solvent, time consumption, significant secondary waste, expensive, sophisticated equipment, and laborious procedures.[3] Magnetic micro-solid phase extraction (Mμ-SPE) was developed as an alternative to the SPE method due to its remarkable properties that could potentially outperform SPE. Benefits of Mμ-SPE include a straightforward process, easy separation, affordability, high efficiency, rapidity, minimal organic solvent use, and the elimination of any filtration or centrifugation steps necessary for sample preparation.[3,10,13–16] This method does not rely on packing the sorbent into the cartridge, and it is simple to isolate the phase separation by using an external magnetic field.[15] The mass transfer is accelerated by the uniform adsorbent dispersion into the sample solution during Mμ-SPE, and the surface area of interaction between the adsorbents and analyte was enhanced.[14] As a result, the extraction process takes less time and has lower toxicity.

To achieve a sufficient recovery of the target analyte *via* Mμ-SPE, an appropriate sorbent choice is vital. Iron oxides such as magnetite (Fe_3O_4) were employed as magnetic nanoparticles (MNPs) due to their great characteristics, including simple preparation methods and effectiveness in separating target analytes from samples, which are frequently used as sorbents.[11,15] Even with the large volume of samples, the use of MNPs greatly reduces extraction time and mass sorbent consumption.[17,18] They guarantee high extraction capacity, dynamic extraction, and extraction efficiency.[11] Even though MNPs have great characteristics, unmodified MNPs are unstable in an acidic medium; thus, different strategies can be used to change the surface of MNPs through modifications to overcome these restrictions.[19,20] Many waste products from industrial and agricultural processes can be used again to create more value for more affordable and efficient adsorbents.[18,20] A "low-cost" adsorbent is one that generally requires little processing, exists abundantly in nature, or is a by-product or waste product from another industry.[21,22]

In Malaysia, due to the high consumption and demand for tea-related products, there is an enormous amount of tea waste generated every year.[22] Based on a literature review, on average, Malaysia produces 0.45% of the world's total tea production. In general, the waste created from making tea is an oxygen-demanding contaminant that takes ample time to degrade.[22,23] On the other hand, Malhotra and co-workers have proved that tea waste functions as a powerful adsorbent for the extraction of pharmaceutical pollutants from water samples.[22] Numerous functional groups on the surface of the tea residue serve as potential pollutant-binding sites.[24] Due to their separation efficiency, increased surface area, efficiency in mass transfer, and chemical stability, magnetic tea waste was synthesized successfully from biomass and has gained a lot of interest. Carboxylate, aromatic carboxylate, phenolic hydroxyl, and oxyl groups are the possible major, responsible functional groups available in this material. Concerning metal ions, organic bases, and other substances such as acidic and anionic chemicals, the poly-model structure of cellulose-based materials exhibits rather significant physicochemical adsorption.[25,26]

The efficiency of tea waste impregnated with magnetic nanoparticles as a low-cost active adsorbent in extracting IBP from an aqueous solution is described in this research under various conditions.[22,26–28] The use of MNP-TW for the analysis of IBP has not been explored much, even though numerous studies have focused on the removal studies.[25,28]

Hence, this work demonstrates the application of the magnetic micro-solid phase extraction (Mμ-SPE) technique of tea waste impregnated with magnetic nanoparticles (MNP-TW) for the microextraction of ibuprofen (IBP) in water samples prior to spectrophotometric analysis. MNP-TW-μ-SPE lowers the consumption of solvent and is biodegradable, time-saving, simple, rapid, and cost-effective.[27,29] Comprehensive optimization was performed on the extraction parameters, including adsorbent dosage, extraction time, ionic strength, type of desorption solvent, desorption time, desorption solvent volume, sample volume, and sample pH. MNP-TW-μ-SPE was effectively used under ideal circumstances to extract IBP from water samples.

Experimental

Chemicals and reagents

Black tea leaves were purchased from a supermarket in Shah Alam, Selangor. The IBP drug was purchased from Aldrich. Table S1† shows the properties of IBP, with their chemical formula, molecular weight, and molecular structures. Fig. S1A† shows the absorption of the UV-Vis spectra when 500 μg L^{-1} of IBP spiked in a solution screened at 222 nm wavelength. Solvents used, such as acetonitrile and methanol, were of HPLC grade (99.7%) and were purchased from Merck (Darmstadt, Germany). Iron(II) chloride tetrahydrate ($FeCl_2 \cdot 4H_2O$) and iron(III) chloride hexahydrate ($FeCl_3 \cdot 6H_2O$) were obtained from

R&M Chemicals (Essex, UK). Sodium chloride (NaCl) and sodium hydroxide (NaOH) were provided by Friedemann Schmidt (Parkwood, WA, Australia). The ultrapure water with a resistivity of >18.2 MΩ was prepared by the Merck Milli-Q system (Lane End, UK). The stock standard solution (1000 mgL^{-1}) was prepared in methanol and stored in a refrigerator. The working standard solutions were freshly prepared by diluting the stock solutions with ultrapure water to the desired concentration.

Instruments

A Shimadzu (Kyoto, Japan) Model UV-1650 UV-Vis spectrophotometer was used for the measurement of IBP. The morphology, dimensions, magnetic characteristics, and composition of the sorbents produced were investigated through various analytical techniques. A vibrating sample magnetometer (VSM, Lake Shore/7404, Lake Shore Cryotronics, Ohio, USA), transmission electron microscopy (TEM, Phillips, CM12 Version 3.2), and field emission scanning electron microscopy with energy dispersive X-ray spectroscopy (FESEM-EDX, Quanta FEG 650) were employed for this purpose. Additionally, the specific surface area, pore volume, and size of the adsorbents were determined using BET analysis of nitrogen adsorption–desorption isotherms at 77.350 K with a Micromeritics instrument (ASAPTM 2020, Georgia, USA). Fourier transform infrared (FT-IR) spectra (Nicolet, Thermo Fisher Scientific) were obtained between 4000 and 400 cm^{-1} using the KBr technique in absorption mode with 32 scans. Thermogravimetric analysis (TGA4000, PerkinElmer Waltham, MA, USA) was conducted to assess weight loss as a function of temperature and time, with samples heated from 30 to 900 °C at a rate of 10 °C min^{-1} under a nitrogen atmosphere. A vortex mixer (LMS, Japan) was used as a supporting apparatus to desorb the analyte from the sorbent to the eluent solvent. An orbital shaker, (SKU: 719, from TECH-LAB) was used for the extraction of IBP from the aqueous solution. The pH values of the sample solutions were determined by a pH meter (Hanna instrument).

Synthesis of MNP-TW

The black tea leaves were used to mix tea beverages, and the residue was collected and soaked in boiled water a few times until decolourized. The residue was thoroughly washed with water and dried at 85 °C overnight.[23,26] Once dried, the material was ground and sieved. Then, the chemical co-precipitation technique was employed, where 11.68 g of ferric chloride and 4.3 g of ferrous chloride were dissolved in distilled water. Under N_2 conditions, the mixture was heated at 80 °C with vigorous stirring at 2000 rpm for 1 hour. N_2 gas was continuously bubbled to expel oxygen gas. After 1 hour, 10 mL of 30% ammonia solution was added dropwise. The solution was then added to 5 g of the fine tea waste material. The reaction was carried out for 30 min at 80 °C under constant stirring. To eliminate unreacted chemicals, the suspension was cooled down to room temperature and washed repeatedly with distilled water. Lastly, the material was washed with ethanol to enhance the crystal formation and dried in an oven overnight at 50 °C for 12 hours. Eqn (1) and (2) show MNP-TW material formation, which was inspired by Panneerselvam and co-workers[26] and tested with the magnet as shown in Fig. 1. It was clear that the MNP-TW was attracted to the magnet due to its magnetic properties.

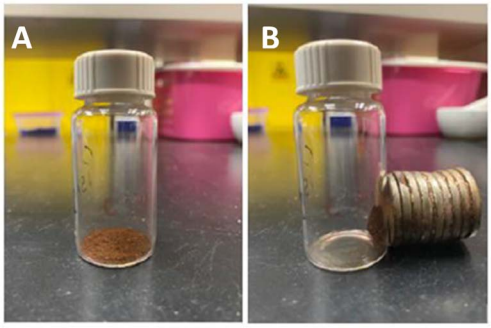

Fig. 1 (A) The image of MNP-TW before being attracted to an external magnetic force by a neodymium magnet. (B) The image of MNP-TW after being attracted to an external magnetic force by a neodymium magnet.

$$FeSO_4 \cdot 7H_2O + 2FeCl_3 \cdot 6H_2O + 8NH_4O \rightarrow Fe_3O_4 + 6NH_4Cl + (NH_4)_2SO_4 + 17H_2O \quad (1)$$

$$Fe_3O_4 + TW + 17H_2O \rightarrow TW - Fe_3O_4 \quad (2)$$

Water samples

Water samples were collected by using pre-cleaned one-liter glass amber bottles from hospital effluent at Universiti Malaya Medical Centre (UMMC), Petaling Jaya, Selangor, and tap water from the Chemistry Laboratory Building, University Malaya, Kuala Lumpur. Samples were collected, stored in a cooler box, and transported to the laboratory. On arrival at the laboratory, any suspended solid particles were removed by continuously passing through a 0.45 μm nylon filter membrane. The water samples were then kept in the refrigerator at 4 °C before analysis. For the recovery test, a suitable quantity of reference solutions containing IBP at three different levels of concentration (100, 400, and 700 μg L^{-1}) was spiked into the water samples.

Magnetic tea waste micro-solid phase extraction procedure

A 10 mL sample solution containing known concentrations of IBP was placed in a vial. Then 20 mg of synthesized MNP-TW material were added to the aqueous solution. The mixture was shaken on an orbital shaker at 1000 rpm for 15 minutes to encourage the analytes to bind to the MNP-TW. The residue with the adsorbed analyte particles was separated by a neodymium magnet. No centrifugation or any time-consuming isolation step was required since the neodymium magnet was perfect for separating the MNP-TW from the aqueous solution. To elute the adsorbed analyte from the surface of MNP-TW, 1.0 mL of desorption solvent was used and held on a vortex for 30 seconds. After the vortex, again with the

aid of a neodymium magnet, the desorption solvent was decanted and diluted in 3 mL of solvent to ensure the cuvette cell volume was sufficiently filled. The solution was then analyzed by UV-Vis spectrophotometer at 222 nm to obtain the extraction recovery. A similar procedure was run for the blank samples and standard solutions to plot a calibration curve.

Results and discussion

Characterization

Fourier transform infrared analysis. The FTIR spectra of MNP-TW, MNP, and TW between 4000 and 400 cm^{-1} are presented in Fig. 2. The spectra display several absorption peaks, reflecting the complex nature of tea waste. By comparison, for MNP-TW, MNP and TW, the troughs due to bonded OH groups are observed in the range of 3340–3380 cm^{-1}. A broad band at 3409 cm^{-1}, 3406 cm^{-1}, and 3384 cm^{-1} from TW spectra is attributed to the presence of bonded (–OH) groups, whereas at (2930–2842 cm^{-1}) and (2931–2850 cm^{-1}), it is attributed to the aliphatic (C–H) groups, which might probably be from the tea waste. The peaks between 1630 cm^{-1} and 1057 cm^{-1} represent C═O stretching mode conjugated with the NH_2 (Amide 1 band) in MNP-TW, representing the carboxylic group and stretching of polysaccharides, indicating the presence of a great amount of carboxylic acid. The skeletal vibrations of C═C stretching (aromatic rings) at 1630 cm^{-1} with the hydroxyl group in MNP-TW and TW are a representation of the large content of polyphenols in MNP-TW. The stretching vibration of the Fe–O bond was responsible for the transmittance band at 634 cm^{-1}. Additionally, the reduced intensity of Fe–O suggested that MNP-TW composites had a significant TW loading. The peaks in the spectra of MNP and TW coincided with those of MNP-TW, proving that MNP-TW nanoparticles were successfully formed.[24,28,30,31]

Magnetization studies

The predominant characteristic of a magnetic material lies in its magnetic properties, which are essential for the rapid separation of materials from an aqueous medium, especially in magnetic micro-solid phase extraction (Mμ-SPE) applications. The magnetic behavior of MNP-TW and MNP was assessed using a VSM (vibrating sample magnetometer), as displayed in Fig. 3. It was discovered that MNP and MNP-TW had saturation magnetizations (M^s) of 62.51 and 40.47 emu g^{-1}, respectively. The difference in the magnetization values of both MNP-TW and MNP yielded 22.04 emu g^{-1}, which is 35.3% (w/w), which was close to that of weight loss calculated from thermogravimetric (TG) analysis (~31.6% in w/w). Thus, this further proved that the synthesis was successful.[10,28] Fig. 3 shows the saturation magnetization (M^s) of MNP and MNP-TW.

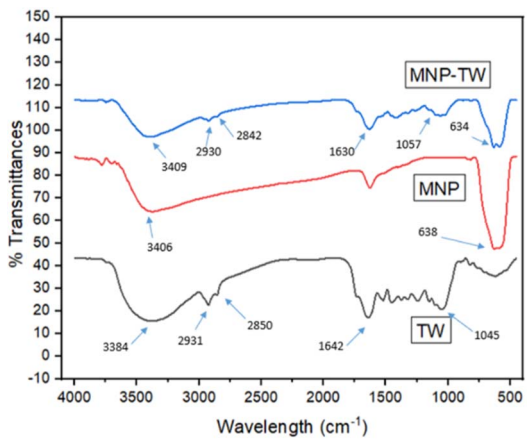

Fig. 2 The FT-IR spectra of MNP-TW, MNP, and TW.

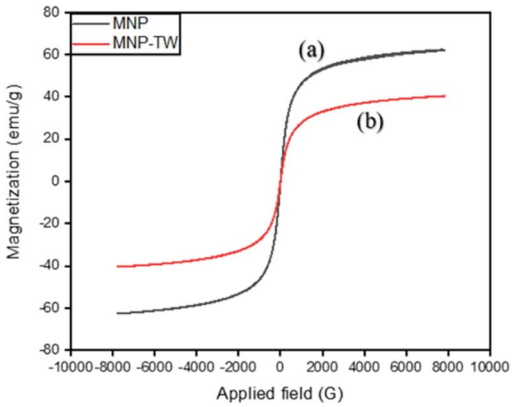

Fig. 3 VSM analysis of (a) MNP and (b) MNP-TW.

Morphology studies: field emission scanning electron microscopy, transmission electron microscopy, Brunauer–Emmett–Teller analysis. FESEM and TEM images for TW, MNP, and MNP-TW were taken to observe the particle surface both before and after TW modification. In Fig. S1(B)(i),† the parent TW has smooth, heterogeneous, irregular, bumpy-structured surfaces. It indicates TW is primarily composed of structural proteins derived from cellulose and has insoluble cell walls with a fibrous composition. As there are more adsorption sites, this feature would help to increase the extraction efficiency. In Fig. S1(B)(ii),† the MNP surface has more pores and compact particles with rough morphology. It adhered closely together, which caused the nanoparticles to aggregate. In MNP-TW, MNP has completely covered the parent TW, as shown in Fig. S1(B)(iii),† and all the MNP particles have aggregated to create a spherical, cage-like structure. Since the iron oxide occupied the active sites, Fig. S1(B)(iii)† depicts a single TW fibrous material with more holes and active sites available at 1.00 μm.

In TEM analysis, the particles of individual MNP and MNP-TW were difficult to visualize. Therefore, their mean particle size was determined by randomly choosing the observed particle grains in the TEM image and plotting the particle size distribution histogram with the aid of ImageJ software. From Fig. S2(A)(i) and S2(A)(ii),† the average diameter obtained from the plot for MNP (15.1 nm) is higher compared to MNP-TW (9.6 nm). The reduction in the average diameter of nanoparticles from MNP to MNP-TW is due to the infusion of MNP into the surfaces and pores of the tea waste during the synthesis, which

was essential for an effective magnetic separation to occur. A similar observation was reported by Wen and co-workers.[28] Further impregnation on the surface of tea waste produced nanoparticles with tiny, spherical morphology.[26,28,32]

In BET analysis, the porous structures of MNP and MNP-TW were studied by using nitrogen adsorption–desorption isotherms. The unmodified MNP (67.14 $m^2\ g^{-1}$) yielded a BET surface higher than MNP-TW (48.38 $m^2\ g^{-1}$). The decline in values could be attributed to the increment in particle diameter due to the presence of an impregnation layer from magnetic nanoparticles on the surface of tea waste.[25,33]

The Barret–Joyner–Halenda model (BJH) was used to calculate the pore size distribution, which gave pore diameters of 13.1 nm and 17.8 nm for MNP and MNP-TW, respectively. These findings align with the IUPAC classification, which categorizes mesoporous materials within a diameter range of 2–50 nm. The increase in pore size could potentially be attributed to the presence of an impregnation layer derived from magnetic nanoparticles. This layer might have contributed to the dimensional enlargement of particles, thereby confirming the successful synthesis of the investigated materials.

Fig. S2(A)(i) and (ii)† show the hysteresis loop of MNP and MNP-TW respectively. In Fig. S2(A)(i)† the MNP displayed a type IV isotherm with an H1-type hysteresis loop, indicative of its mesoporosity. The outcomes are in line with the SEM analysis, whereby porous material that exhibited type H1 contained uniform sphere aggregates. However, in Fig. S2(A)(ii),† MNP-TW demonstrated type II with an H3-type hysteresis loop, which indicates the formation of a monolayer on the material's surface. This behavior is said to be common for materials with relatively low surface areas, where multilayer adsorption occurs after monolayer adsorption. The H3-type hysteresis loop observed in Type II isotherms signifies the presence of a macroporous surface with relatively uniform cylindrical mesopores or ink-bottle-shaped pores in MNP-TW. While mesoporous and macroporous materials differ in their pore size ranges, they can sometimes be related to certain materials. For example, a material could exhibit a hierarchical porous structure containing both mesopores and macropores. This combination of different pore sizes might be advantageous, providing multiple levels of adsorption capabilities for different-sized molecules or particles.[13,26,34] Table S2† presents the BET results of MNP and MNP-TW.

X-ray diffraction analysis. As shown in Fig. S3(A),† the analysis of crystallinity was carried out using X-ray powder diffraction (XRD) spectroscopy. The typical peaks of pristine MNP were found to correspond to the Miller index values of (220), (311), (400), (422), (511), and (440) planes of MNP with a face-centered cubic structure at $2\Theta = 30.3°$, 35.7°, 43.3°, 53.8°, 57.4°, and 63.1°, respectively. (JCPDS No. 75-0033). The two patterns showed a broad and relatively weak diffraction peak at 23°, which indicates the amorphous carbon consists of aromatic carbon sheets oriented in a relatively random manner.[35] It should be observed that the impregnation process of MNP on tea waste did not alter the cubic phase of the magnetic particles, as shown by the identical XRD pattern of MNP-TW. The results obtained from Fig. S3(A),† can be used to determine the crystallite sizes of MNP and MNP-TW with the Scherer equation in eqn (3).

$$D = k\lambda/\beta \cos \Theta \tag{3}$$

where D is crystalline size,[36] k is grain shape factor constant, λ is the wavelength of the XRD beam, β is the full width at half maximum for the diffraction peak (radian), and Θ is the diffraction angle.

The quantitative analysis based on the Scherer equation showed that the average crystallite sizes of MNP and MNP-TW are 14.1 nm and 11.4 nm, respectively. As can be realized, the crystallite size of MNP-TW is lower than the size of MNPs achieved by BET and TEM techniques.

Thermogravimetric analysis. The thermal stability of a molecule is measured by thermogravimetric analysis (TGA), which is also employed to analyze MNP and MNP-TW. According to Fig. S3(B)(i),† the weight-loss curve for MNP and MNP-TW required a multi-step approach. In general, the first step can be understood because of the loss of water, while the second step may be responsible for other compounds. Upon increasing the temperature to 200 °C, the weight of MNPs was reduced by 3.69%, apparently caused by the loss of moisture content. However, only a minor loss in weight (2.50%) occurred at temperatures ranging from 200 °C to 400 °C due to minor volatile fractions, with the remaining MNP purity obtained at 93.81%. For MNP-TW, a three-step degradation pattern was obtained. The first step involved a loss of 5.96% moisture content at temperatures <200 °C, followed by a 13.22% reduction in weight between 200 °C and 400 °C in the second step, which is attributed to the loss of cellulose and hemicellulose residues as well as volatile fractions. In the third step, a loss in weight of 12.45% was observed at 400 °C to 800 °C, accounting for the devolatilization of thermally stable volatile compounds, the oxidation of carbon, and the degradation of lignin. A final residue mass of 68.37% was obtained.[25] Fig. S3(B)(ii)† provides additional evidence of that of MNP and MNP-TW. The findings are summarized and displayed in Table S3.†

Optimization of magnetic micro-solid phase extraction conditions preliminary studies (comparison between magnetic nanoparticles and magnetic tea waste)

The extraction performance of MNP-TW and native MNP was examined in the extraction of IBP using similar extraction conditions ($n = 3$), which included 20 mg of sorbent, 10 mL of sample solution, 30 min of extraction time, 30 s of desorption time, and 1.0 mL of acetonitrile as the desorption solvent. This experiment was conducted to ascertain the impact of tea-waste modification on the sorbents' ability to extract materials. Fig. S3(C)† displays the measured absorbance of IBP applying MNP and MNP-TW. According to the bar chart, MNP-TW demonstrated a higher extraction efficiency, which can be attributed to the tea waste impregnated with magnetic nanoparticles, which increased the porosity of the adsorbent and drew more IBP particles toward it.[26] Additionally, the polyphenol compound in tea waste, which contains functional groups such as hydroxyl groups, carboxyl groups, and benzene

rings in its structure, enhances selectivity for IBP and adds another outstanding characteristic to the interaction system. Furthermore, the greater extraction capability of MNP-TW towards the studied IBP could be due to strong π–π interaction and electrostatic interaction.[19]

Effect of sorbent dosage. The amount of MNP-TW in the range of 5–30 mg was evaluated, with other conditions kept unchanged. As shown in Fig. S4(i),† the optimum amount was 25 mg. When the amount of MNP-TW increases, the extraction efficiency increases too. MNP-TW provides a large surface area, which facilitates strong adsorption for their π–π electrostatic interactions with the aromatic rings of the targets, which explains the adsorption capacity variation and thus the limited number of active sites.[37] However, the extraction efficiency decreases after 25 mg due to particle aggregation that happens when a high mass of adsorbent is present, which reduces the surface area of MNP-TW exposed to IBP for the adsorption to occur.[32,38]

Effect of pH. The FT-IR spectrum in Fig. 2 demonstrates the presence of carbonyl, hydroxyl, and carboxyl functional groups on the surface of MNP-TW. The oxygen-bonded functional groups enhance the affinity of the MNP-TW with the analyte, making the magnetic materials suitable for extraction. It also acts as a hydrogen bond donor and acceptor. The target IBP analyte and the adsorbent's present forms, as well as the charge species and the associated density on the adsorbent surface, are all significantly influenced by the pH values of water samples.[38] The impact of pH values in the range of 3 to 11 was investigated and presented in Fig. S4(ii).† At pH 4, it was found that maximum extraction efficiency was achieved. It might be explained by the significant hydrogen bonding and hydrophobic interactions between MNP-TW and IBP. IBP has a dissociation constant (pK_a) value of 4.52. At pH < 4, the solution is rich in hydrogen ions, H^+, making the polar IBP prone to protonation. The protonation effect impedes the hydrogen bonding interaction and thus weakens the adsorption. At optimum pH 4, near the pK_a value, IBP exists in molecular form. The hydrogen bonding interaction is the strongest, leading to optimal adsorption. When pH > 5, IBP changed to anionic forms, and the MNP-TW became electroneutral or even negatively charged, thus resulting in reduced interaction and repulsion.[39,40] Since IBP would be ionized and present in their conjugated forms at a sample pH greater than their pK_a values, an increase in the sample pH bigger than 4 led to a gradual fall in the extraction recovery.[40] To prepare the sample solution for further analysis, the pH was adjusted to 4 for subsequent analyses.[10,19]

Effect of extraction time. The length of the extraction process has a significant impact on how IBP is distributed between the aqueous phase and the MNP-TW adsorption sites, which helps to increase extraction efficiency. Equilibrium is reached when the sorbent can extract the most analyte possible. To obtain the best extraction efficiency, the extraction time was investigated. The time required for analyte diffusion into a thicker sorbent was greater than for thinner materials. The effect of different extraction times (10–60 min) was studied at room temperature, as shown in Fig. S4(iii).† The extraction efficiency was greater for IBP at 10 min, then decreased. Therefore, the optimum extraction time for IBP was 10 min, which was selected for further experiments.[41]

Effect of ionic strength. The effect of ionic strength was studied to determine if ionic strength could improve the performance of this method. An ionic strength of 0–5% of NaCl is added to the sample solution. As shown in Fig. S4(iv),† the optimum ionic strength was 0% (no addition) of NaCl, which was selected for further experiments. When NaCl is added to samples, the solution's viscosity rises and the diffusion coefficient falls, which is bad for extraction. The high density and viscosity of the solution may prevent IBP from transferring its molecular mass to the sorbents. Therefore, in the following trials, no NaCl was added to the sample solution. Additionally, at high salt concentrations, Na^+ and Cl^- ions reversed the metathesis reaction to make MNP-TW more polar. This slowed the pace at which IBP diffused from the aqueous to the MNP-TW because the IBP's solvation cage was broken.[3,42] As such, the extraction performance declined. Therefore, further experiments were carried out without the addition of NaCl 0% (w/v).

Effect of sample volume. The sample volume correlates directly with both the MNP-TW's loading capacity and enrichment factor (EF). The sample volume was tested in the range of 5 to 30 mL to obtain a high enrichment factor. In Fig. S4(v),† results indicate that IBP prefers lower sample volumes. From 10 to 30 mL, the trend seemed to decrease. Due to the high dispersion of MNP-TW in aqueous solutions, greater amounts result in the adsorption sites becoming entirely saturated with IBP, making it impossible to process the sample. The adsorption of IBP is now more challenging. As a result, 10 mL was selected as the optimum sample volume for the proposed method.[39]

Effect of desorption solvent. In the case of MNP-TW-μ-SPE, IBP was desorbed by a polar organic solvent from the surface of MNP-TW after extraction. Different desorption solvents were evaluated (methanol, acetonitrile, and acetone). As shown in Fig. S4(vi),† the best desorption solvent for IBP was acetonitrile. The affinity of the desorption solvent towards IBP depends on the solvent polarity and the solubility in the solvent. The selected polar solvents have higher solvent strengths. This result might be explained by the fact that IBP mostly lived in nonionic forms in acidic environments.[40]

Effect of desorption time. The vortex method was employed in the desorption process. To ensure complete desorption, the desorption time was tested in the range of 10 to 50 s. As shown in Fig. S4(vii),† for IBP, the analytical signals achieved their optimum when the desorption time was fixed at 20 s. For 20 s, the duration allowed the complete desorption of IBP from the MNP-TW material surface. The decrease seen after 20 seconds may be the result of the IBP re-desorbing from the MNP-TW over a longer duration. Thus, the adsorbed IBP can be quantitatively stripped from the magnetic sorbent by desorption under the vortex.

Effect of desorption volume. The influence of desorption volume on the desorption of IBP from MNP-TW was studied from 200 to 1000 μL. According to Fig. S4(viii),† IBP prefers 800 μL as the ideal volume of desorption to elute the analyte from the MNP-TW adsorbent, which produces the maximum

extraction from the sorbent. The low desorption volume (<1 mL) further contributes to the microextraction concept and further illustrates that better extractions can be made by employing smaller volumes, which enhances higher extraction performance.

To sum up, based on the overall outcomes, the optimum extraction parameters were finally selected and are presented in Table S4.†

Sorbent reusability study

After considering how important it is for the environment to reduce waste and save chemicals, the feasibility of reusing MNP-TW was investigated. For this reusability investigation, the same MNP-TW that had undergone three complete washings with 1.5 mL of acetonitrile each and a 30 minutes drying period at 65 °C was employed. As presented in Fig. S5(A),† results show that there was no analyte carryover throughout the MNP-TW-μ-SPE procedure and that the MNP-TW could be reused up to 2 times (>70%) (*as per ICH guidelines for analytical method validation*) with a signal that remained virtually constant. The MNP-TW potential for reuse in the real MNP-TW-μ-SPE application was proved in this way.

Analytical performance/validation of the proposed magnetic micro-solid phase extraction method. Under the optimized conditions, the linearity, limit of detection (LOD), limit of quantification (LOQ), precision, pre-concentration factor (PF), and sorbent reproducibility were studied and presented in Table S5† to validate the analytical performance of the proposed MNP-TW-μ-SPE coupled with UV-Vis spectrophotometry. A series of spiked samples that ranged between 30 and 700 μg L^{-1} were applied to plot the calibration graph ($n = 3$) obtained by plotting the absorbance signal against the concentrations of IBP following the standard MNP-TW-μ-SPE technique. IBP exhibited linearity with satisfactory determination coefficients (R^2) of 0.9983. The LOD was defined as LOD = 3.3 s m^{-1}, while the LOQs were denoted as LOQ = 10 s m^{-1} (s is the standard deviation of blank residuals, and m is the slope of the calibration graph). The LOD was 9.40 μg L^{-1}, whereas the LOQ was 28.50 μg L^{-1}. It is interesting to note that the values of LOD and LOQ for some NSAIDs were comparable or appeared to be better than those achieved by other methods, as presented in Table 1.

The reproducibility of the method was determined by evaluating the intra-day (repeatability on the same day, $n = 10$) and inter-day (6 different days, $n = 3$) precisions by spiking water samples at 300 μg L^{-1}. Satisfactory precisions were obtained with relative standard deviation (RSD) values of 1.48% and 1.53% for intra-day and inter-day, respectively, illustrating the good reproducibility achieved by the MNP-TW-μ-SPE method.

Under optimal MNP-TW-μ-SPE conditions, the PF value for IBP at a spiked level of 300 μg L^{-1} was obtained as 116

Sorbent reproducibility study

The MNP-TW synthesis repeatability was assessed in terms of batch-to-batch or lot-to-lot reproducibility. The extraction efficiency of each batch was studied by spiking 500 μg L^{-1} of IBP in water samples employing three batches of sorbents ($n = 3$) that were manufactured under the same conditions but at different times. As shown in Fig. S5(B),† all three batches produce an extraction efficiency of more than 80%, with RSD values of 0.4% to 5.6%. The RSD values appeared to be improved and acceptable. This suggests that the MNP-TW preparation used in this investigation has good repeatability.

Application of real sample analysis. To study the effectiveness of the suggested method for application on real water samples, tap water and hospital effluent water were tested. Water samples were spiked simultaneously with 100, 400, and 700 μg L^{-1} of IBP. All experiments were repeated three times ($n = 3$). Plotting the absorbance signal against the concentration of IBP species exposed to the usual process under optimal conditions resulted in a calibration graph for the concentration range of 30–700 μg L^{-1}. The findings were compiled in Table S6,† where the full recoveries for all IBP species fell between 86 and 115%. As a result, the technique can be regarded as extracting IBP from water samples.

Fig. S5(C)† shows a typical UV-Vis spectrum obtained from a water sample spiked with IBP at 50 μg L^{-1} and 100 μg L^{-1} evaluated with and without the MNP-TW-μ-SPE technique and compared with an unspiked sample. This indicates that the matrix effect did not have any significant effect on the recovery of the spiked analyte. In addition, it shows the effectiveness of the MNP-TW-μ-SPE to enrich the IBP in water samples.

Interference study

The challenge of the matrix effect arises significantly when analyzing trace levels of pharmaceuticals in water samples

Table 1 Comparison of the analytical performance of the method developed with other extraction methods in the literature[a]

Extraction method	Analyte	Linear range (μg L^{-1})	LOD (μg L^{-1})	Instrument	Pre-concentration factor	Recovery (%)	Reference
Mμ-SPE (modified with arginine amino acid)	DCF	50–10000	39	UV-Vis	—	92.0–100.8	46
MSPE (modified with carbon nanodots)	ERY	100–500	60	UV-Vis	6.7	94.8–97.6	14
UADSPME (molecularly imprinted polymer)	CAR	100–1200	33	UV-Vis	25	97.0–112.0	17
MNP-TW-μ-SPE	IBP	30–700	9.4	UV-Vis	116	86.0–115.0	This work

[a] MSPE = magnetic solid phase extraction; Mμ-SPE = magnetic micro-solid phase extraction; MNP-TW-μ-SPE = magnetic tea waste micro-solid phase extraction; UADSPME = ultrasound-assisted dispersive solid phase microextraction; IBP = ibuprofen; DCF = diclofenac; ERY = erythrosine; CAR = carbaryl; LOD = limit of detection; UV-Vis = ultraviolet-visible spectrophotometer.

using magnetic micro-solid phase extraction (Mμ-SPE) in combination with spectrophotometric determination methods. Consequently, a study was conducted to investigate how interferences affect the anticipated spectrophotometric response to IBP, considering the presence of potential interfering pharmaceutical compounds commonly found in environmental samples. Sample solutions spiked with 100, 400, and 700 μg L^{-1} of IBP were spiked with 1 mL of 500 μg L^{-1} diclofenac and naproxen, each in different combinations. All samples were then extracted under optimized experimental conditions. The spike combinations and results are given in Table S7.† Notably, some of these commonly occurring species in environmental samples did not disrupt the current spectrophotometric method. Hence, it can be inferred from these findings that there are no significant interferences by other NSAIDs near the IBP wavelength, affirming the good selectivity of the developed method towards IBP.

Green assessment. The analytical Eco-Scale has been selected as an innovative, all-encompassing tool to assess how environmentally friendly the analytical methodology is. It is assessed using the penalty points deducted for analytical process variables that do not support the notion of "green analysis." This method contrasts variations in the analytical process's phases and parameters. The volumes of chemicals/reagents, the energy used by electrical equipment, the potential occupational hazards, and the waste product produced by this approach, as stated in Table S8,† all contributed to the penalty points. Based on the reagents' level of risk, which includes their hazards, according to the Globally Harmonized System of Classification and Labeling of Chemicals (GHS), penalty points are allotted.[43–45]

If the amount of chemical is <10 mL (g), 1 penalty point is assigned, while 2 penalty points are given for reagent amounts between 10 and 100 mL (g). In addition, the hazard penalty also considers a reagent's warning or danger signal. The MNP-TW-μ-SPE method and its functional materials were used to calculate the penalty points for synthesis from raw tea, and the result was 24 penalty points. Ammonia (25%) has been classified with the warning signal word according to GHS data, resulting in a penalty of 6 points. Other mentioned chemical solvent usage, in the meantime, has been designated with the signal word "danger" and the corresponding penalty points.[44,45]

The total energy consumption contributed to 4 penalty points. Zero penalty points are contributed by UV-Vis due to 0.1 kW h of energy per sample being consumed, and the other 2 penalty points are for each stirrer and orbital shaker during material synthesis that consumed an average of 1.5 hours. Five penalty points were recommended for waste generation where >10 mL of waste was produced during the material synthesis and extraction process. The occupational hazards hold 3 penalty points. Altogether, 24 penalty points were accumulated, and the net value was deducted from 100 points, which were the total ideal green scores. Therefore, the total AES score is 76, which shows the MNP-TW-μ-SPE method for the determination of IBP in water samples is neatly a green analysis (acceptable green analysis >50 points).[45]

Comparison with other literature. To evaluate the performance of the method based on MNP-TW-μ-SPE, the present method was further compared with the reported methods involving other extraction techniques and adsorbents using UV-Vis spectrophotometric analysis, and the details are listed in Table 1. The preparation of MNP-TW adsorbent in the proposed method is simple and rapid; there were no specific or expensive reagents involved in the reactions, while other studies used some expensive, specific reagents that were complicated to synthesize. Some studies have used commercial sorbent that is easy to use but costly. It is a good choice for the development of adsorbents following the principle of green analytical chemistry. It must be noted that not many extraction methods are employed with UV-Vis spectrophotometry analysis. Moreover, among the listed works, not many studies have chosen waste material for the development extraction method for the detection of IBP, coupled with UV-Vis spectrophotometry analysis. The MNP-TW-μ-SPE technique has surpassed the previous record by producing very low LOD and LOQ values, a good preconcentration factor, a wide range of linearity, and better recoveries compared to other studies.

Conclusions

The MNP-TW-μ-SPE method comes with several benefits, including low cost, selectivity, safety, and superior extraction efficiency. As far as we are aware, this is the first study on the application of tea waste impregnated with magnetic nanoparticles (MNP-TW) using Mμ-SPE for the extraction method of the IBP species in water samples. High recoveries can be attained at the optimized parameters, according to experimental results. In this study, the synthesized MNP-TW and the developed Mμ-SPE technique were demonstrated to be an efficient strategy for rapid extraction of IBP. As a result, it may be used as an alternative or as a routine application for rapid and precise IBP analysis in water samples.

Author contributions

Yagulan Muniandy: writing—original draft, methodology, investigation, formal analysis. Sharifah Mohamad, Muggundha Raoov: supervision, funding acquisition, writing—review and editing.

Conflicts of interest

The authors declare that they have non-related competing financial interests or personal relationships that could have appeared to influence the work reported in this paper.

Acknowledgements

The work is supported financially by the Ministry of Higher Education Malaysia *via* the Fundamental Research Grant Scheme (FRGS/1/2019/STG01/UM/02/16) for their financial support of this work. The authors would also like to seize this

opportunity to express their gratitude to the Department of Chemistry, Faculty of Science, and Universiti Malaya.

References

1 S. Bindu, S. Mazumder and U. Bandyopadhyay, *Biochem. Pharmacol.*, 2020, **180**, 114147.
2 A. Eslami, M. M. Amini, A. R. Yazdanbakhsh, N. Rastkari, A. Mohseni-Bandpei, S. Nasseri, E. Piroti and A. Asadi, *Environ. Monit. Assess.*, 2015, **187**, 734.
3 T. Wang, S. Liu, G. Gao, P. Zhao, N. Lu, X. Lun and X. Hou, *Microchim. Acta*, 2017, **184**, 2981–2990.
4 A. Sebok, A. Vasanits-Zsigrai, G. Palko, G. Zaray and I. Molnar-Perl, *Talanta*, 2008, **76**, 642–650.
5 S. F. F. Syed Yaacob, A. K. Mohd Jamil, M. A. Kamboh, W. A. Wan Ibrahim and S. Mohamad, *PeerJ*, 2018, **6**, e5108.
6 N. Abd Rahman, N. H. Hashim, M. H. Nasir, M. S. Ramlee, Z. Mohd Jaini, R. Yunus and S. N. Rahmat, *MATEC Web of Conferences*, 2016, vol. 47.
7 K. Świacka, A. Michnowska, J. Maculewicz, M. Caban and K. Smolarz, *Environ. Pollut.*, 2021, **273**, 115891.
8 Z. Mohd Hanafiah, W. H. M. Wan Mohtar, T. S. B. Abd Manan, N. A. Bachi, N. A. Abdullah, H. H. Abd Hamid, S. Beddu, N. L. Mohd Kamal, A. Ahmad and N. Wan Rasdi, *Chemosphere*, 2022, **287**, 132134.
9 S. Duman, Z. Erbas and M. Soylak, *Microchem. J.*, 2020, **159**, 105468.
10 S. Liu, S. Li, W. Yang, F. Gu, H. Xu, T. Wang, D. Sun and X. Hou, *Talanta*, 2019, **194**, 514–521.
11 M. A. Tarighat, A. Behroozi, G. Abdi and C. Proestos, *Separations*, 2023, **10**, 6334.
12 C. Toledo-Neira and A. Alvarez-Lueje, *Talanta*, 2015, **134**, 619–626.
13 Y. H. Boon, N. N. Mohamad Zain, S. Mohamad, H. Osman and M. Raoov, *Food Chem.*, 2019, **278**, 322–332.
14 E. Emiroğlu, D. Yuvali, G. Sarp, E. Yilmaz and İ. Narin, *Microchem. J.*, 2021, **170**, 106766.
15 S. A. Haeri, S. Abbasi and S. Sajjadifar, *Electrophoresis*, 2017, **38**, 2765–2770.
16 E. Larsson, S. Al-Hamimi and J. A. Jonsson, *Sci. Total Environ.*, 2014, **485–486**, 300–308.
17 A. A. Bazrafshan, M. Ghaedi, Z. Rafiee, S. Hajati and A. Ostovan, *J. Colloid Interface Sci.*, 2017, **498**, 313–322.
18 A. H. Panhwar, T. G. Kazi, H. I. Afridi, S. A. Arain, K. Naeemullah, K. D. Brahman and M. S. Arain, *Spectrochim. Acta, Part A*, 2015, **138**, 296–302.
19 W. Li, R. Wang and Z. Chen, *J. Chromatogr. A*, 2018, **1576**, 19–25.
20 S. F. F. Syed Yaacob, M. A. Kamboh, W. A. Wan Ibrahim and S. Mohamad, *R. Soc. Open Sci.*, 2018, **5**, 171311.
21 M. M. Kabir, S. S. P. Mouna, S. Akter, S. Khandaker, M. Didar-ul-Alam, N. M. Bahadur, M. Mohinuzzaman, M. A. Islam and M. A. Shenashen, *J. Mol. Liq.*, 2021, **322**, 115012.
22 M. Malhotra, S. Suresh and A. Garg, *Environ. Sci. Pollut. Res.*, 2018, **25**, 32210–32220.
23 N. Atirah Mohd Nazir, M. Raoov and S. Mohamad, *Microchem. J.*, 2020, **159**, 105581.
24 S. Wong, Y. Lim, N. Ngadi, R. Mat, O. Hassan, I. M. Inuwa, N. B. Mohamed and J. H. Low, *Powder Technol.*, 2018, **338**, 878–886.
25 B. S. Inbaraj, K. Sridhar and B. H. Chen, *J. Hazard. Mater.*, 2021, **415**, 125701.
26 P. Panneerselvam, N. Morad and K. A. Tan, *J. Hazard. Mater.*, 2011, **186**, 160–168.
27 S. Lunge, S. Singh and A. Sinha, *J. Magn. Magn. Mater.*, 2014, **356**, 21–31.
28 T. Wen, J. Wang, X. Li, S. Huang, Z. Chen, S. Wang, T. Hayat, A. Alsaedi and X. Wang, *J. Environ. Chem. Eng.*, 2017, **5**, 3656–3666.
29 J. W. Drynan, M. N. Clifford, J. Obuchowicz and N. Kuhnert, *Nat. Prod. Rep.*, 2010, **27**, 417–462.
30 F. Liu, X. Yang, X. Wu, X. Xi, H. Gao, S. Zhang, W. Zhou and R. Lu, *Food Chem.*, 2018, **268**, 485–491.
31 M. S. Shahriman, M. R. Ramachandran, N. N. M. Zain, S. Mohamad, N. S. A. Manan and S. M. Yaman, *Talanta*, 2018, **178**, 211–221.
32 S. Bakhshaei, M. A. Kamboh, H. R. Nodeh, S. Md Zain, S. K. Mahmad Rozi, S. Mohamad and I. A. Mohammed Mohialdeen, *RSC Adv.*, 2016, **6**, 77047–77058.
33 A. R. Altaf, H. Teng, M. Zheng, I. Ashraf, M. Arsalan, A. U. Rehman, L. Gang, W. Pengjie, R. Yongqiang and L. Xiaoyu, *J. Environ. Chem. Eng.*, 2021, **9**, 105313.
34 M. Raoov, S. Mohamad and M. R. Abas, *Int. J. Mol. Sci.*, 2014, **15**, 100–119.
35 T. Wen, J. Wang, S. Yu, Z. Chen, T. Hayat and X. Wang, *ACS Sustain. Chem. Eng.*, 2017, **5**, 4371–4380.
36 M. Wu, Z. Xia, Q. Zhang, J. Yin, Y. Zhou and H. Yang, *J. Chem.*, 2016, **2016**, 1–8.
37 E. B. Hsen and L. Latrous, *J. Chromatogr. Sci.*, 2023, **61**, 186–194.
38 A. H. El-Sheikh, R. F. Qawariq and J. I. Abdelghani, *Environ. Technol. Innovation*, 2019, **16**, 100496.
39 V. Manzo, L. Honda, O. Navarro, L. Ascar and P. Richter, *Talanta*, 2014, **128**, 486–492.
40 A. Sarafraz-Yazdi, A. Amiri, G. Rounaghi and H. Eshtiagh-Hosseini, *Anal. Chim. Acta*, 2012, **720**, 134–141.
41 Z. Rezaeifar, Z. Es'haghi, G. H. Rounaghi and M. Chamsaz, *J. Chromatogr. B*, 2016, **1029–1030**, 81–87.
42 X. Han, J. Chen, Z. Li and H. Qiu, *Anal. Chim. Acta*, 2019, **1078**, 78–89.
43 S. Armenta, S. Garrigues and M. de la Guardia, *Trends Anal. Chem.*, 2015, **71**, 2–8.
44 N. N. Zain, N. K. Abu Bakar, S. Mohamad and N. M. Saleh, *Spectrochim. Acta, Part A*, 2014, **118**, 1121–1128.
45 A. Gałuszka, Z. M. Migaszewski, P. Konieczka and J. Namieśnik, *Trends Anal. Chem.*, 2012, **37**, 61–72.
46 H. A. Shahhosseini, S. Heydari, Z. Es'haghi and L. Zare, *J. Iran. Chem. Soc.*, 2021, **19**, 1747–1754.